



Design, fabrication, and structural safety validation of 3D-printable biporous bone augments

Yeokyung Kang^{1,2} · Dasol Lim¹ · Doo-Hoon Sun^{1,3} · Jong-Chul Park² · Jungsung Kim¹

Received: 26 April 2022 / Accepted: 18 September 2022 / Published online: 26 October 2022
© The Author(s) 2022

Abstract

The use of commercial products such as a cup and liner for total hip arthroplasty for patients with severe bone defects has a high probability of failure. In these patients the cup alone cannot cover the bone defect, and thus, an additional augment or cage is required. In this study, we designed three-dimensional (3D) printable bone augments as an alternative to surgeries using reinforcement cages. Thirty-five sharp-edged bone augments of various sizes were 3D printed. A biporous structure was designed to reduce the weight of the augment and to facilitate bone ingrowth. Two types of frames were used to prevent damage to the augment's porous structure and maintain its stability during printing. Furthermore, two types of holes were provided for easy augment fixation at various angles. Fatigue tests were performed on a combination of worst-case sizes derived using finite element analysis. The test results confirmed the structural stability of the specimens at a load of 5340 N. Although the porosity of the specimens was measured to be 63.70%, it cannot be said that the porous nature was uniformly distributed because porosity tests were performed locally and randomly. In summary, 3D-printable biporous bone augments capable of bonding from various angles and bidirectionally through angulation and bottom-plane screw holes are proposed. The mechanical results with bone augments indicate good structural safety in patients. However, further research is necessary to study the clinical applications of the proposed bone augment.

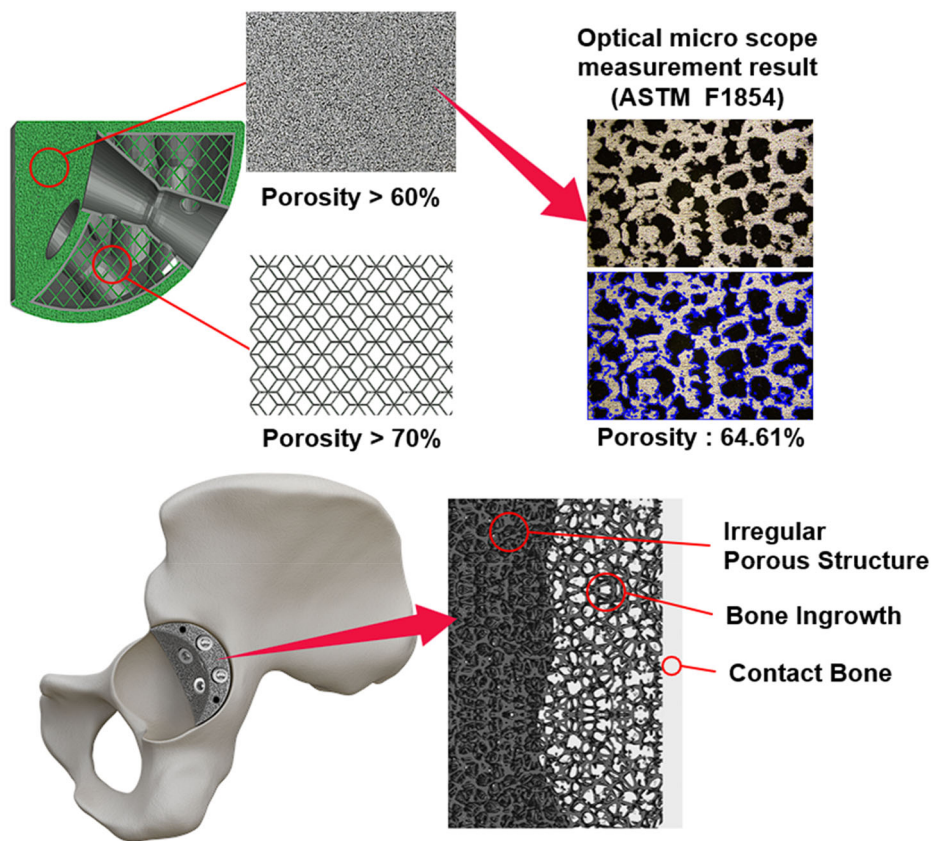
✉ Jungsung Kim
jskim@corentec.com

¹ Central Research & Development Center, Corentec Company Ltd., 33-2, Banpo-daero 20-gil, Seocho-gu, Seoul, Republic of Korea

² Cellbiocontrol Laboratory, Department of Medical Engineering, Yonsei University College of Medicine, 50-1 Yonsei-ro, Sinchon-dong, Seodaemun-gu, Seoul, Republic of Korea

³ Department of Orthopaedic Surgery, Daejeon Sun Hospital, 10-7 Mok-dong, Jung-gu, Daejeon, Republic of Korea

Graphic abstract



Keywords Bone augment · 3D printing · Biporous structure · Total hip arthroplasty · Metal implant

Introduction

The hip joint, formed by the junction of the femur and the pelvis, covered primarily with cartilage total hip arthroplasty (THA), is a treatment for damaged hips wherein an implant is used to replace the damaged joint. Standard metal implants for the pelvis, such as acetabular cups, are commercially available [1–3]. The number of THA cases has reached 28,000 per year in South Korea and 100,000 per year in the USA. Moreover, these numbers are expected to double by the end of 2026 [4–6]. The increasing number of THA cases has led to the development of the acetabular cup implant on a commercial scale. This implant is recommended for patients whose acetabulum is not severely damaged. However, for patients with severe pelvic injuries, including reoperations (resubstitution operations), the large hole in the acetabulum renders surgery using only a regular acetabular cup a challenge [7, 8].

In such patients, surgery using a standard acetabular cup requires the use of bone augments. Acetabular reconstruction in complex, primary hip replacement can present challenges,

and off-the-shelf cages and augments, and, recently, patient-customized implants have been used. Patient-customized implants with a high cost are often used in highly complex scenarios. Conventional treatments for damaged hips include using oblong (bilobed) acetabular components or jumbo acetabular components [9, 10], or covering the damaged area with bone cement [11]. Allograft reoperation using a reinforcement cage has been the gold standard in such patients [12–14]. However, it has been reported that reinforcement cages in allograft reoperation have failed many times over the long-term clinical results of the last 10 years, most often owing to defects in the roof of the pelvis and holes caused by injuries to the pelvis.

Therefore, alternative implants and bone augments are actively studied. Personalized implants offer the advantage of postoperative stability and patient satisfaction because they can be tailored for a perfect fit. However, allografts using reinforcement cages suffer from the disadvantage of a higher surgical cost, approximately 2–3 times that of metal bone augments [15]. In addition, a 2014 Bradford Royal Infirmary study in the UK reported that customized hip-revision

implants had postoperative revision and complication rates of 15.9% and 24.5%, respectively. The corresponding rates for the use of augments were 8.2% and 29.1%. In contrast, the porous metal system augment had low revision and complication rates of 8.5% and 18.5%, respectively, thereby validating the long-term stability of surgeries performed using bone augments [16]. Therefore, this present study aims to design a bone augment and to evaluate the porosity and fatigue resistance, thereby determining the safety and stability of biporous bone augments.

Titanium is used as a material for bone augments because it has been proven to be safe for clinical use in humans. Further, recent developments in three-dimensional printing (3D-printing) technologies have brought 3D-printed products and research results into the spotlight. One advantage of 3D-printing technology is its design for additive manufacturing (DfAM), helping fabricate bone augments of any shape and size, which are otherwise difficult to manufacture using conventional methods. DfAM enables the fabrication of external porous structures for bone augments. Because this 3D-printing technology can fabricate the external appearance of the bone-augment material with a porous structure, the initial fixation of the implant with the bone is enhanced and the contact surface with the bone is widened. These elements enhance the long-term bond between the bone augment and the bone and induce a stable bond by stimulating bone growth [17–22].

A study conducted by the Mayo Clinic and the Mayo Foundation in 2004 examined the clinical results of bone-augment surgeries. The study reported that the Harris hip score increased from an average of 39.31 to 75.19 points in 16 patients who underwent hip-revision surgery with bone augments. The patients were satisfied, except for one, who required a second surgery [23]. Further, in a study performed at the Rush University Medical Center in 2006 on 28 patients, the modified Postel Merle d'Aubigne score improved from 6.8 to 10.6 after an average of 3.1 years, following hip revision with porous structural bone augments [24]. The clinical results confirmed that patients were satisfied with the combination of hip-revision surgery with porous bone augments.

In this present study, bone augments with biporous structures were developed using 3D-printing technology, in which the porosity and thickness of the internal and external surfaces were varied to maximize the functionalization of the augment. The external surface was designed with a porous structure for bone growth, whereas the internal surface was designed with a porous structure to reduce the weight of the augment. Porosity evaluation and fatigue tests were performed to determine the safety and stability of the bone augment.

Bone augment

Design

The shape of the bone augment developed in this study is shown in Fig. 1a. Because the bone augment was used in conjunction with an acetabular cup implant during surgery, a sharp edge was designed (Fig. 1b) to enhance its adhesion with the cup. Further, as depicted in Fig. 1c, if the edge of the bone augment is round, a gap exists between the acetabular cup implant and the bone augment. Consequently, there may be microscopic movement of the contact surface, resulting in gaps at the contact point with the bone. Therefore, the augment was designed with a sharp-edge form to minimize these problems.

The bone augment in this study was designed with two types of holes: bottom-plane and angulation screw holes. A variety of screw angles were used to improve the fixation between the acetabular cup and the pelvis, as depicted in Fig. 2a. To enable screw insertions in various directions, the bottom-plane and angulation screw holes were designed to provide screw angles of 11°–14° and 17°–24°, respectively (Figs. 2b and 2c). The holes were shaped similarly to an hourglass such that screws could be inserted from various angles, regardless of the position of the augment insertion, according to the bone loss.

Two types of frames were used for the bone augment. An edge-frame structure was designed, as shown in Fig. 3, to prevent damage to the printed support and porous structure of the augment during 3D printing. In 3D printing, a common practice is to set a support on the bed and to place the specimen on it. Therefore, the porous structure is damaged if a dome edge is not used in the design. Moreover, in the event that the porous structure form is combined with a 3D-printing support, the porous structure may become damaged when the support is removed. Therefore, inner and outer dome edges were designed. The edge domes were designed with different lengths to maximize the preservation of the shape of the porous structure.

The bone augment comprised two different types of porous structures (Fig. 4). In the first type, an irregular porous structure was used to ensure the stability of the implant and to induce long-term bone regeneration by increasing the contact area with the bone. The area between the acetabular cup and the bone augment was filled with bone cement to increase the stability of the joint. In contrast, in the second type, a regular porous structure was used to function as a framework for the bone augment while minimizing its weight.

As depicted in Fig. 4, a 1.5-mm-thin wall frame was designed to act as a boundary between the irregular and regular porous structures to prevent structural instability that might occur during 3D printing owing to the irregular

Fig. 1 Hip-augment design: **a** augment shape, **b** sharp edge, and **c** smooth edge

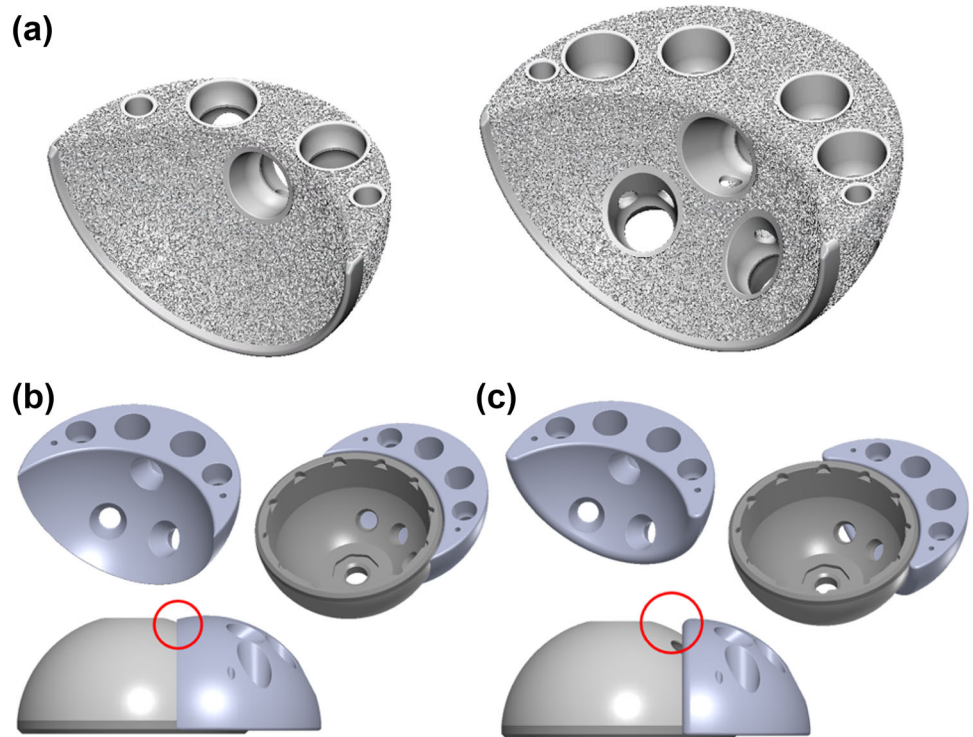
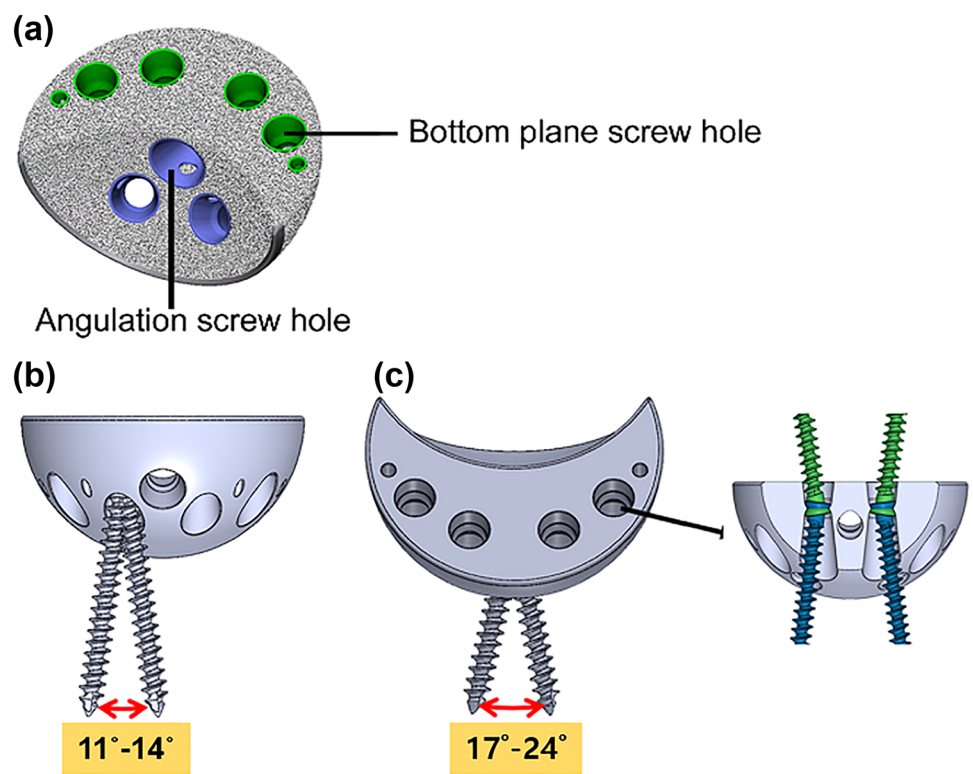


Fig. 2 **a** Angulation screw hole and bottom-plane screw hole, **b** bottom-plane screw hole, and **c** angulation screw hole



arrangement of the two porous structures. The connectivity of the two porous structures was considered as well.

Size

The size of the developed bone augment was determined based on the compatibility of the hip-replacement system

Fig. 3 **a** Inner-dome-edge frame and **b** outer-dome-edge frame

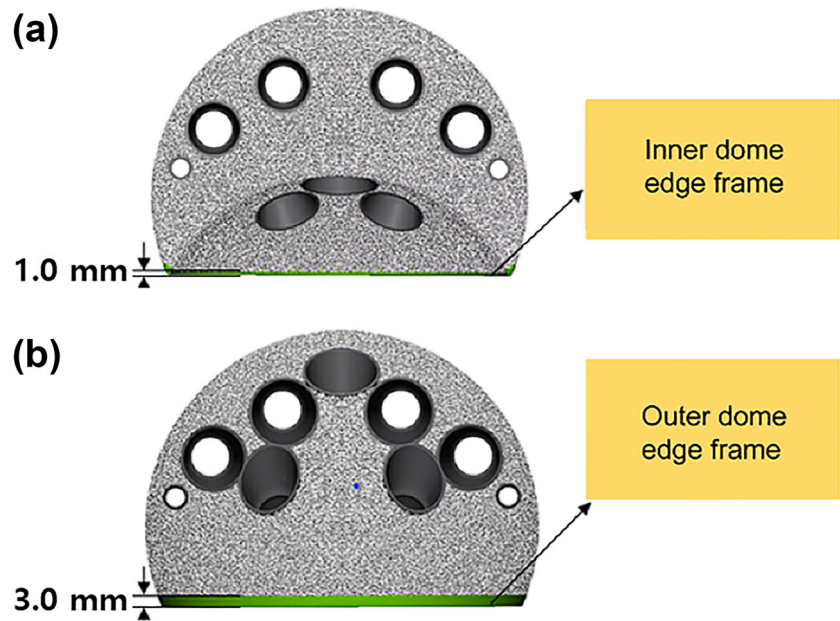


Fig. 4 Thin-wall frame at the biporous contact point

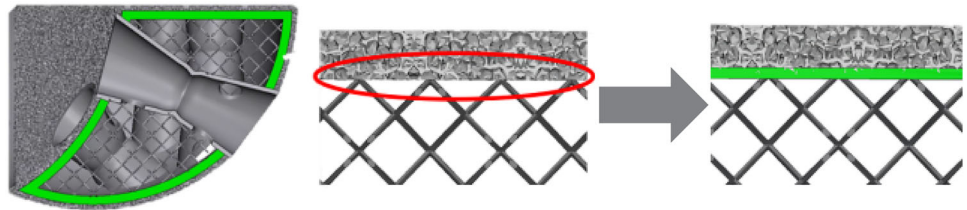
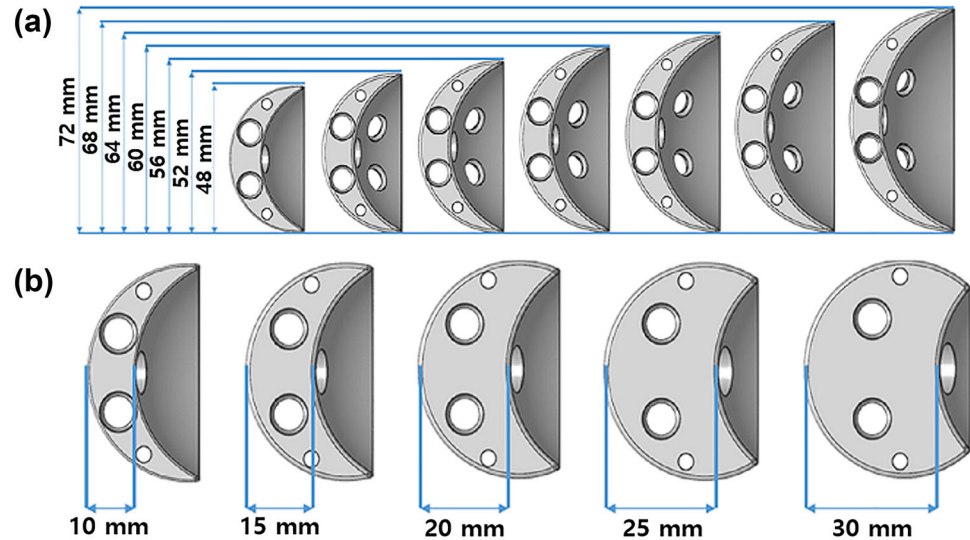


Fig. 5 Augment: **a** outer diameter and **b** thickness



with the acetabular cup. Seven different sizes for the outer diameter of the bone augment were designed at increments of 4 mm within a 48–72 mm range (Fig. 5a); five different values of the thickness were designed at increments of 5 mm within a 10–30 mm range (Fig. 5b); and a total of 35 different sizes were designed. Further, the hip-replacement system was designed to be compatible with the acetabular cups sold in

South Korea. The sizes were selected in consideration of the specifications required for surgery. In the areas where the hip-replacement system and augment did not fit perfectly, the gaps were filled with bone cement at the joint interface.

Fig. 6 **a** Outer irregular structure and **b** inner regular structure

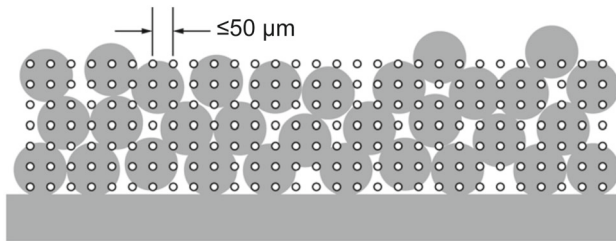
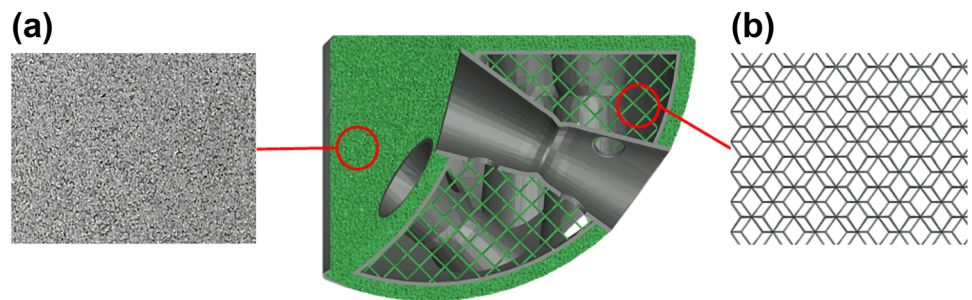


Fig. 7 Illustration of volume percent void measurement [26]

Structure

Biporous structure

As is evident from Fig. 6, two types of porous structures were integrated into the bone augment. An irregular porous structure was applied to the outer surface of the bone augment where porous contact with the bone or acetabular cup occurred from all directions of insertion. The high surface roughness at the bone contact area improved the initial fixation to the bone, thereby facilitating mechanical fixation. In addition, the area in contact with the bone was set at 1 mm thick with a porosity of 60% or higher to induce bone growth and to enhance postoperative biological-fixation capacity [25].

The porous structure within the bone augment was designed to have a regular morphology. This structure was designed to reduce weight while supporting the load-bearing capacity of the bone augment. Moreover, the structure was designed to maximize the amount of free space by setting the porosity to 70% or higher. A fatigue test was performed to confirm the structural safety of the augment.

Safety and stability tests

Porosity test

The porosity method given in Fig. 7 was used according to the ASTM F1854 standard to measure the porosity of the designed augment. The bone augment was fabricated using the powder-bed fusion method, and pure titanium material

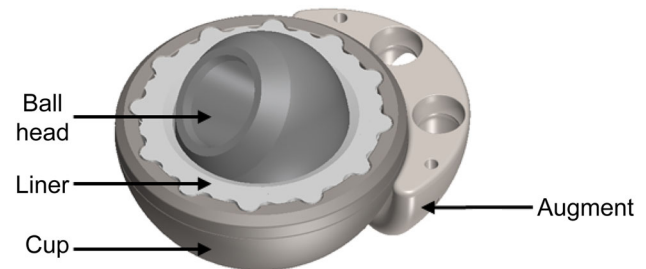


Fig. 8 Combined model for finite element analysis (FEA)

was cut by machine processing to measure its cross section. Thereafter, an optical microscope (OLYMPUS Co., Ltd., BX53M) was used to magnify the cross section of the bone augment at 2.5 times magnification for the porosity measurement test. The porosity was determined from the cross-sectional image obtained with the optical microscope using ImageJ (National Institutes of Health, USA). The program includes a built-in function for determining the porosity using Eq. (1). The porosity tests were repeated for four bone-augment samples.

$$P_v = \frac{P_a}{P_T} \times 100\%, \quad (1)$$

where P_v represents the volume percent void, P_a represents the total number of counted points, and P_T represents the total number of grid points.

Fatigue test

Worst-case selection

The designed bone augment was subjected to fatigue tests to assess the mechanical safety of its biporous structure. For these tests, a worst-case model was selected using finite element analysis (FEA), which was performed using the static analysis in Ansys (Ansys, Inc., USA).

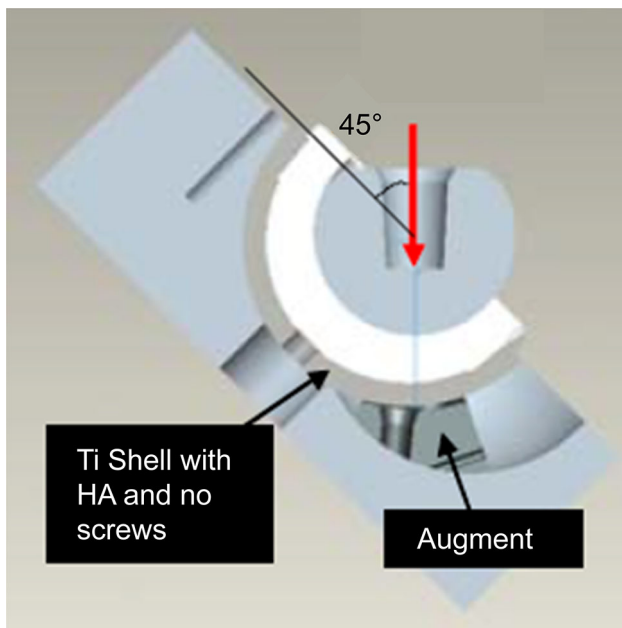
The ball-head, liner, and cup followed by the bone augment were combined with the hip-replacement system to develop a model for the analysis, as shown in Fig. 8. In the combined model, bonded contact conditions were added to the entire contact surface, and a setting was added to ensure

Table 1 Specifications of the combined models

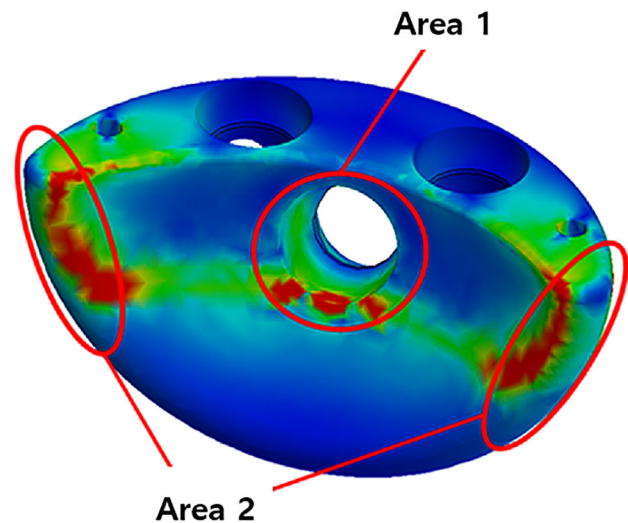
Specimen no.	Cup	Augment	Liner	Ball head
#1	48 mm	Diameter: 48 mm Thickness: 10 mm	28/39 mm	28 mm (S)
#2				28 mm (M)
#3				28 mm (XL)
#4				28 mm (XL_Skirted)
#5				28 mm (XXL)
#6	72 mm	Diameter: 72 mm Thickness: 10 mm	36/62 mm	36 mm (S)
#7				36 mm (M)
#8				36 mm (XXL)
#9				40 mm (S)
#10			40/62 mm	40 mm (M)
#11				40 mm (XXL)

Table 2 Mechanical properties for finite element analysis (FEA)

Part	Material	Elastic modulus (GPa)	Poisson's ratio	Density (kg/m ³)	Yield strength (MPa)
Ball head	CoCr alloy	210	0.29	10,000	1600
Liner	UHMWPE	1.2	0.46	940	27.6
Cup	Ti6Al4V	113.8	0.342	4430	790
Augment	Pure titanium	105	0.37	4510	410

**Fig. 9** Load conditions for finite element analysis (FEA) (HA: hip arthroplasty)

that the gap in the contact was smaller than 0.5 mm. Load was applied as depicted in Fig. 9. Further, based on the study by Fuchs in 2011, the model was developed by coupling a 72-mm acetabular cup model of the highest specification with a 10-mm-thick augment, which was also the thinnest model in the 48-mm acetabular cup model (Table 1) [27]. Accordingly, the liner and ball-head specifications were selected.

**Fig. 10** Peak von-Mises stress (PVMS) measurement areas

The ball head was subdivided into S–XXL sizes based on the stem insertion depth. The skirted model was a raised spot on the part in contact with the stem. Table 2 summarizes the mechanical properties of each material for the coupled models. Bond-contact conditions were added to the interfaces of each coupled model. In the event of an equal load being applied to all coupled models regardless of their magnitude, a 5 N load was used to identify the worst case. The peak von-Mises stress (PVMS) values were measured for all the models and were compared. In addition, the PVMS values

Table 3 Porosity test results

Sample	Porosity (%)	Pore size (μm)	Strut thickness (μm)
#1	62.81	648.93	263.72
#2	64.98	658.71	261.59
#3	63.22	639.75	265.49
#4	63.79	651.23	262.15
Average	63.70	649.65	263.24

observed in the two areas where stresses were concentrated (Fig. 10) were measured.

Test method

The fatigue test procedure was as follows. As depicted in Figs. 11a and 11b, the bone augment was fixed to a UHMWPE jig using 35-mm screws, and the acetabular cup was bonded to the UHMWPE jig and bone augment using polymethylmethacrylate (PMMA) bone cements. Subsequently, the cup was fixed to the UHMWPE jig using 15-mm screws, and the liner was attached to the cup using the metal head (Fig. 11c). Thereafter, the sample was attached to the base of the solution tank, as shown in Fig. 11d. Further, a taper adaptor was used to attach the metal head to the hydraulic actuator, and an axial load of 5340 N was applied over a frequency of 15 Hz, with 10,000,000 cycles per six samples. Additionally, the magnitude of the load was adapted from the hip–stem–fatigue–test standard (ASTM F7206-6).

Results

Porosity test

The results of the porosity tests are given in Fig. 12 and Table 3. The 3D-printing method produced a thicker structure, which meant that the values had to be adjusted to increase the pore size. Therefore, the average porosity was calculated to be 63.70%, which was higher than the designed porosity of 60%. The average pore size and strut thickness were 649.65 and 263.24 μm , respectively.

Fatigue test

Worst-case selection results

The results of FEA for the worst-case selection are summarized in Fig. 13 and Table 4. The highest PVMS values in measurement areas 1 and 2 were 705,900 and 214,200 Pa, respectively. Both were measured on the XXL-sized ball-head model. However, because the relevant ball-head speci-

Table 4 Results of the worst-case finite element analysis (FEA)

Specimen no.	Combined model list	PVMS (Pa)	
		Area 1	Area 2
#1	48_48/10_28/39_28 (S)	298,300	170,400
#2	48_48/10_28/39_28 (M)	325,900	157,800
#3	48_48/10_28/39_28 (XL)	323,500	145,500
#4	48_48/10_28/39_28 (XL_skirted)	349,900	163,000
#5	48_48/10_28/39_28 (XXL)	705,900	150,100
#6	72_72/10_36/62_36 (S)	8803	88,860
#7	72_72/10_36/62_36 (M)	5853	159,400
#8	72_72/10_36/62_36 (XXL)	962.5	214,200
#9	72_72/10_40/62_40 (S)	1700	141,600
#10	72_72/10_40/62_40 (M)	6086	103,100
#11	72_72/10_40/62_40 (XXL)	9630	129,900

fications are based on models for which there is no actual demand and which are not produced, the highest PVMS value within the range of actual ball-head specifications was determined considering the Specimen #4 model. Because the Specimen #4 model measured 349,900 and 163,000 Pa in measurement areas 1 and 2, respectively, this model was selected as the worst case.

Fatigue test results

The results of the fatigue test are summarized in Table 5. All six bone-augment samples that were tested underwent 10,000,000 cycles with a load of 5340 N without damage (Fig. 14). There was no debris in the augment samples, which confirms the structural stability of the bone augment.

Discussion

The objective of this study was to design a 3D-printable bone augment with a biporous structure and to analyze its structural stability and safety. A sharp edge was designed for the bone augment to increase its adhesion within the hip-replacement system, minimize the gap between the acetabular cup and the bone augment, and minimize the microscopic motion of the contact surface. Furthermore, two types of holes were drilled in the bone stiffener to improve the fixation force between the hip-replacement system and pelvis. In clinical applications, a design that can be in close contact with the bone and a hole angle that can allow diversely inserted screws improves the fixation force between the bone and augment.

As a biporous structure, the bone augment was designed with outer irregular and inner regular structures. Its outer

Fig. 11 Fatigue test setup: **a** prepared sample with cup-liner and screw, **b** prepared sample (full view), **c** liner seating setup, and **d** hip-augment construct fatigue test setup

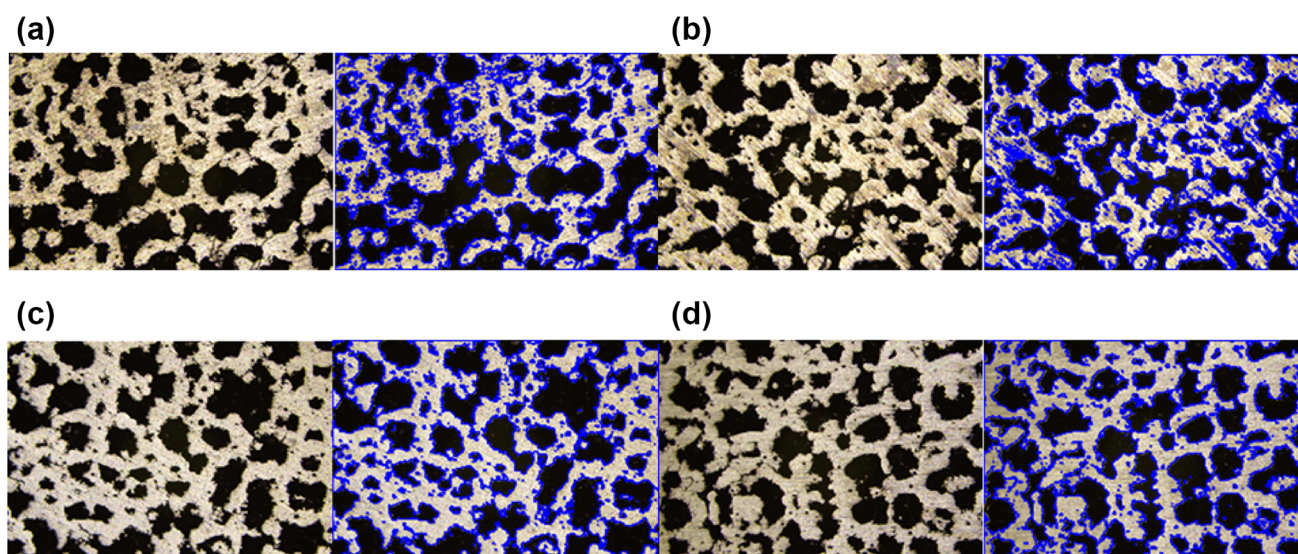
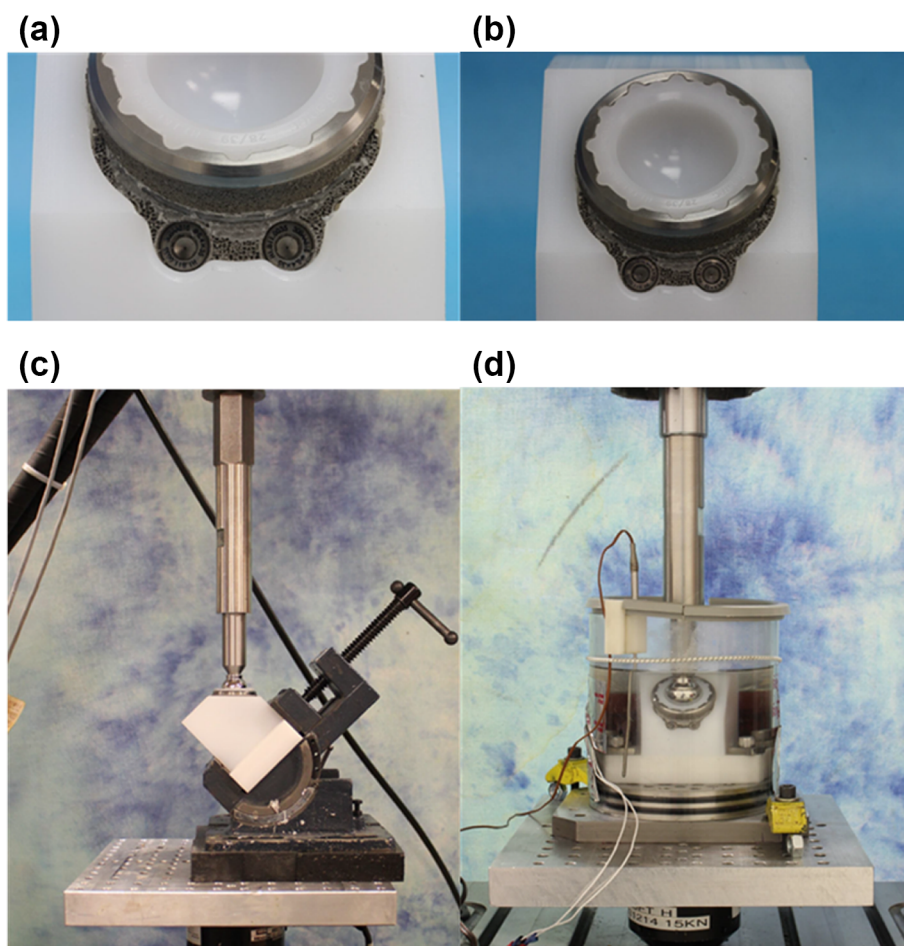


Fig. 12 Porosity test results: **a** Sample #1, **b** Sample #2, **c** Sample #3, **d** Sample #4

irregular structure is in contact with the bone to increase the roughness of the surface, thereby improving initial fixation, inducing bone growth, and maintaining long-term fixation after surgery, whereas, through the application of the inner

regular structure, the inside of the bone augment is hollowed to reduce its weight and improve its manufacturing stability.

Porosity was also evaluated during fabrication to ensure that the structure was manufactured according to design spec-

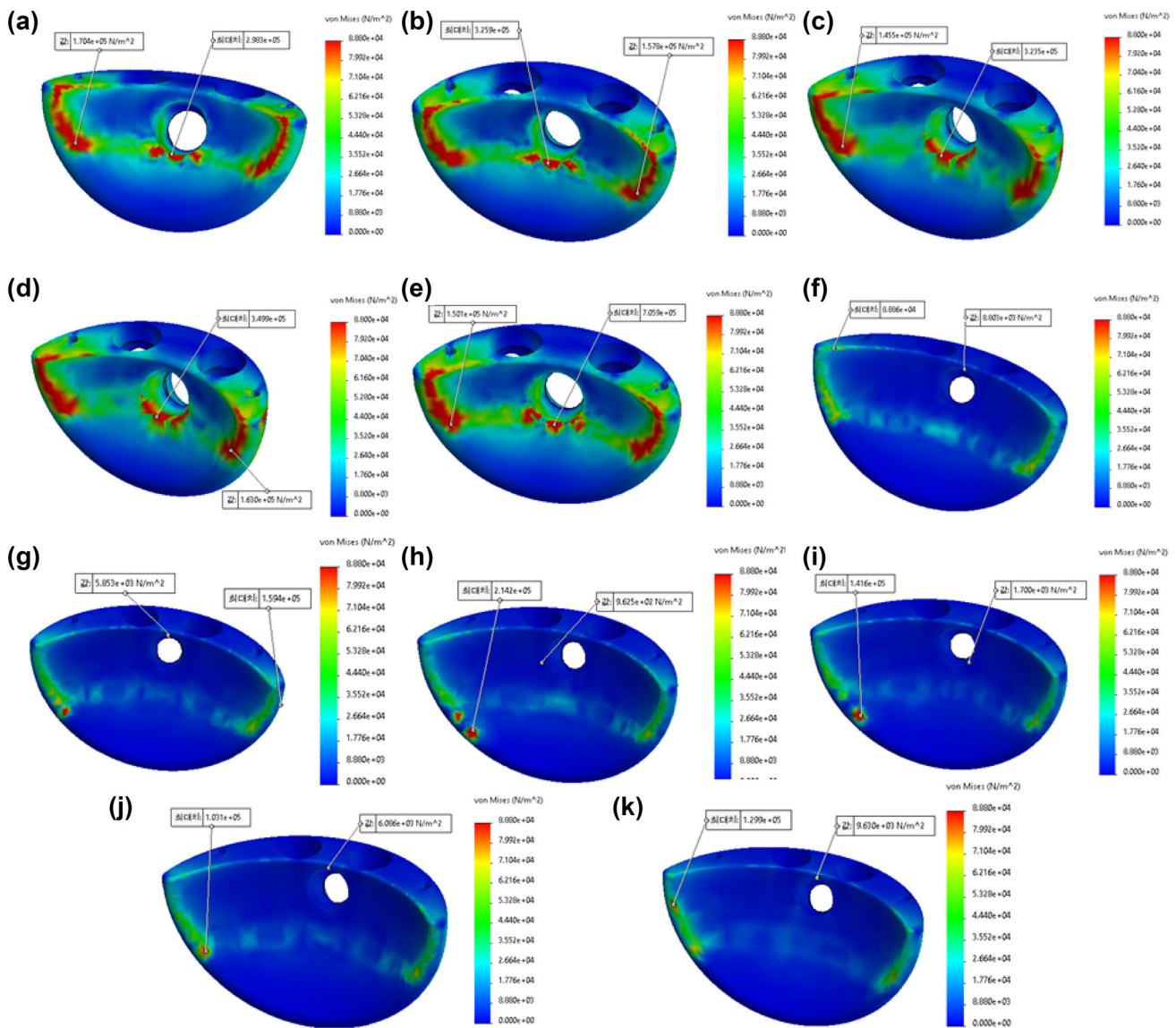


Fig. 13 Results of finite element analysis (FEA) for worst case: **a** Specimen #1, **b** Specimen #2, **c** Specimen #3, **d** Specimen #4, **e** Specimen #5, **f** Specimen #6, **g** Specimen #7, **h** Specimen #8, **i** Specimen #9, **j** Specimen #10, and **k** Specimen #11

ifications. In tests conducted based on ASTM F1854, an average porosity of 63.70% was obtained, indicating that the target porosity of 60% or higher was achieved. When the porous structure for bone ingrowth is over 50%, optimal bone growth can occur. Thus, the obtained average porosity of 63.70% is highly significant because the higher it is, the more bone growth induction can be increased [28, 29].

The bone augment designed in this study is characterized by its biporous structure. Although the proposed augment is functionally similar to other existing bone augments, its biporous structure is intended to reduce the weight of the implant and promote bone growth. Achieving these twin objectives is not possible with a uniporous design. If the porous structure is intended to reduce the weight of the

implant, the hip-replacement system will not be sufficiently strong and will cause problems during its mechanical fixation with the bone. In contrast, if the porous structure is designed with the objective of stimulating bone growth, the pore spaces are then smaller, and the weight of the implant increases. Thus, we used a biporous structure in this study to improve the twin objectives of weight reduction and the bone growth induction of the implant.

The limitations of this study are as follows. Although the porosity of the porous structure was measured to be 60%, there is no evidence indicating a uniform distribution of the porous structure in the bone augment, due to the test being locally conducted at random locations. Random locations are because the 3D-printing conditions may cause variations

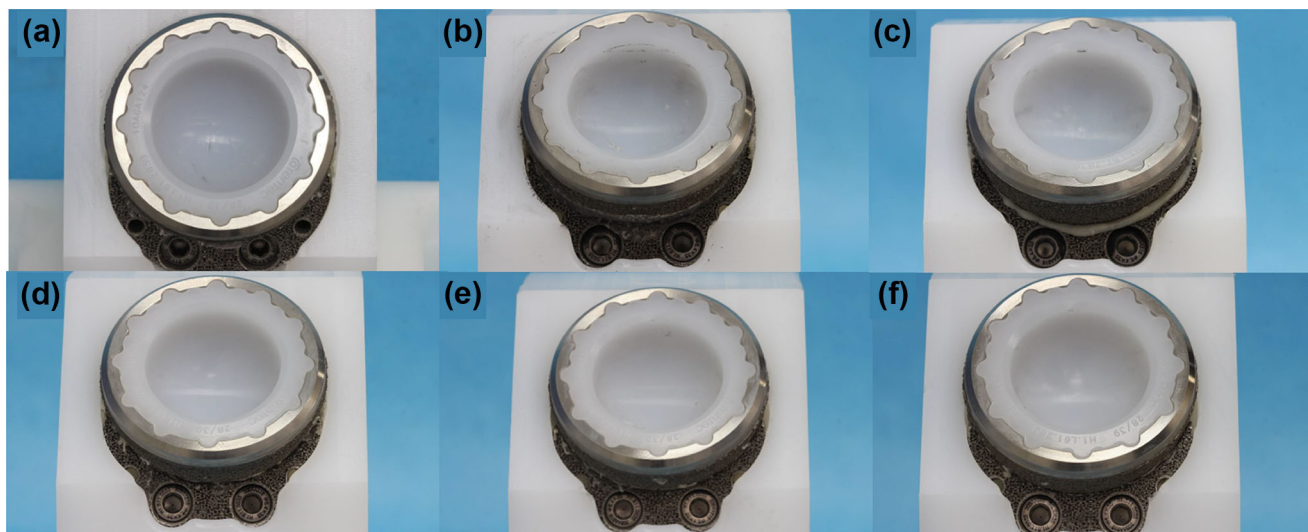


Fig. 14 Fatigue test samples after the test: **a** Sample #1, **b** Sample #2, **c** Sample #3, **d** Sample #4, **e** Sample #5, **f** Sample #6

Table 5 Fatigue test results

Sample	Test load (N)	Cycles achieved	Result
#1	5340	10,000,000	Runout, no visible fractures or dissociation
#2		10,000,000	Runout, no visible fractures or dissociation
#3		10,000,000	Runout, no visible fractures or dissociation
#4		10,000,000	Runout, no visible fractures or dissociation
#5		10,000,000	Runout, no visible fractures or dissociation
#6		10,000,000	Runout, no visible fractures or dissociation

in local porosity. Therefore, further studies are required to validate the advantages of the proposed augment [26, 30].

Conclusions

In this study, we used 3D-printing technology to fabricate bone augments with a biporous structure for total hip arthroplasty. We performed porosity and fatigue tests to evaluate and validate the structural safety and durability of the fabricated bone augments. To proceed further in this research direction, user evaluation of the proposed bone augment

is necessary to confirm its clinical application in total hip arthroplasty.

Acknowledgements We wish to acknowledge Coretec, an implant specialist company, for the help with creating the artworks for this study. This work was supported by the Technology Development Program (P0011350) funded by the Ministry of SMEs and Startups (MSS, Korea).

Author contributions YK was a major contributor to the conceptualization, methodology, formal analysis and manuscript preparation. DL performed a writing review and editing. JCP, DHS and JK contributed to project administration and reviewed the overall. JK was direction of this study and was the final approver of the overall review and manuscript writing. All authors have read and approved the final manuscript.

Declarations

Conflict of interest The authors declare that they have no conflict of interest.

Ethical approval This study does not contain any studies with human or animal subjects performed by any of the authors.

Open Access This article is licensed under a Creative Commons Attribution 4.0 International License, which permits use, sharing, adaptation, distribution and reproduction in any medium or format, as long as you give appropriate credit to the original author(s) and the source, provide a link to the Creative Commons licence, and indicate if changes were made. The images or other third party material in this article are included in the article's Creative Commons licence, unless indicated otherwise in a credit line to the material. If material is not included in the article's Creative Commons licence and your intended use is not permitted by statutory regulation or exceeds the permitted use, you will need to obtain permission directly from the copyright holder. To view a copy of this licence, visit <http://creativecommons.org/licenses/by/4.0/>.

References

- Eftekhari NS (1993) Total hip arthroplasty (vol 1). Mosby, Missouri. ISBN 9780801616693 (ISBN10: 0801616697). https://books.google.co.kr/books/about/Total_Hip_Arthroplasty.html?id=wV9sAAAAMAAJ&redir_esc=y
- Amstutz HC (1991) Hip arthroplasty. Churchill Livingstone, New York
- Van HJ, Khanduja V, Pattyn C et al (2017) The history of biomechanics in total hip arthroplasty. *Indian J Orthop* 51(4):359–367. https://doi.org/10.4103/ortho.IJOrtho_280_17
- Kim SM, Kim Y (2019) National health insurance statistical yearbook. Published by Health Insurance Review & Assessment Service, National Health Insurance Service. ISSN 1738–8945 (in Korean)
- Steiner C, Andrews R, Barrett M, et al (2012) HCUP projections report (2012–03). U.S. Agency for Healthcare Research and Quality, Rockville
- Weber M, Witzmann L, Wieding J et al (2019) Customized implants for acetabular Paprosky III defects may be positioned with high accuracy in revision hip arthroplasty. *Int Orthop* 43(10):2235–2243. <https://doi.org/10.1007/s00264-018-4193-3>
- Alejandro Gonzalez Della Valle, MD (2016) Revision total hip replacement: an overview. Hospital for Special Surgery. https://www.hss.edu/conditions_revision-total-hip-replacement-overview.asp
- Kim HJ, Kim JS, Han SM et al (2009) Evaluation of mechanical stability in development of customized hip implant. *J Kor Soc Precis Eng* 26(7):31–37 (in Korean)
- Moskal JT, Higgins ME, Shen J (2008) Type III acetabular defect revision with bilobed components. *Clin Orthop Relat Res* 466(3):691–695. <https://doi.org/10.1007/s11999-007-0079-1>
- Dearborn JT, Harris WH (2000) Acetabular revision arthroplasty using so-called jumbo cementless components: an average 7-year follow-up study. *J Arthroplasty* 15(1):8–15. [https://doi.org/10.1016/s0883-5403\(00\)90999-9](https://doi.org/10.1016/s0883-5403(00)90999-9)
- Tsai SW, Chen CF, Wu PK et al (2018) Cement augmentation in the proximal femur to prevent stem subsidence in revision hip arthroplasty with Paprosky type II/IIIa defects. *J Chin Med Assoc* 81(6):571–576. <https://doi.org/10.1016/j.jcma.2017.11.008>
- Moussa A, Rahman S, Xu M et al (2020) Topology optimization of 3D-printed structurally porous cage for acetabular reinforcement in total hip arthroplasty. *J Mech Behav Biomed Mater* 105:103705. <https://doi.org/10.1016/j.jmbm.2020.103705>
- Gerber A, Pisan M, Zurakowski D et al (2003) Ganz reinforcement ring for reconstruction of acetabular defects in revision total hip arthroplasty. *J Bone Joint Surg* 85(12):2358–2364. <https://doi.org/10.2106/00004623-200312000-00013>
- Whitehouse MR, Masri BA, Duncan CP et al (2015) Continued good results with modular trabecular metal augments for acetabular defects in hip arthroplasty at 7 to 11 years. *Clin Orthop Relat Res* 473(2):521–527. <https://doi.org/10.1007/s11999-014-3861-x>
- Migaud H, Common H, Girard J et al (2019) Acetabular reconstruction using porous metallic material in complex revision total hip arthroplasty: a systematic review. *Orthop Traumatol Surg Res* 105(1):S53–S61. <https://doi.org/10.1016/j.otsr.2018.04.030>
- Jain S, Grogan RJ, Giannoudis PV (2014) Options for managing severe acetabular bone loss in revision hip arthroplasty. A systematic review. *Hip Int* 24(2):109–122. <https://doi.org/10.5301/hipint.5000101>
- Wyatt MC (2015) Custom 3D-printed acetabular implants in hip surgery—innovative breakthrough or expensive bespoke upgrade? *Hip Int* 25(4):375–379. <https://doi.org/10.5301/hipint.5000294>
- Zanasi S, Zmerly H (2020) Customised three-dimensional printed revision acetabular implant for large defect after failed triflange revision cup. *BMJ Case Rep* 13(5):e233965. <https://doi.org/10.1136/bcr-2019-233965>
- Woo SH, Sung MJ, Park KS et al (2020) Three-dimensional-printing technology in hip and pelvic surgery: current landscape. *Hip Pelvis* 32(1):1–10. <https://doi.org/10.5371/hp.2020.32.1.1>
- Park JW, Shin YC, Kang HG et al (2021) In vivo analysis of post-joint-preserving surgery fracture of 3D-printed Ti-6Al-4V implant to treat bone cancer. *Bio-Des Manuf* 4(4):879–888. <https://doi.org/10.1007/s42242-021-00147-2>
- Wang Z, Wang C, Li C et al (2017) Analysis of factors influencing bone ingrowth into three-dimensional printed porous metal scaffolds: a review. *J Alloys Compd* 717:271–285. <https://doi.org/10.1016/j.jallcom.2017.05.079>
- Wang Z, Yao R, Wang D et al (2021) Structure design and biological evaluation of the mechanical-adaptive titanium-based porous implants. *Mater Technol* 36(14):851–856. <https://doi.org/10.1080/10667857.2020.1800306>
- Nehme A, Lewallen DG, Hanssen AD (2004) Modular porous metal augments for treatment of severe acetabular bone loss during revision hip arthroplasty. *Clin Orthop Relat Res* 429:201–208. <https://doi.org/10.1097/01.blo.0000150133.88271.80>
- Sporer SM, Paprosky WG (2006) The use of a trabecular metal acetabular component and trabecular metal augment for severe acetabular defects. *J Arthroplasty* 21(6):83–86. <https://doi.org/10.1016/j.arth.2006.05.008>
- Kienapfel H, Sprey C, Wilke A et al (1999) Implant fixation by bone ingrowth. *J Arthroplasty* 14(3):355–368. [https://doi.org/10.1016/s0883-5403\(99\)90063-3](https://doi.org/10.1016/s0883-5403(99)90063-3)
- ASTM F1854-15 (2016) Standard test method for stereological evaluation of porous coatings on medical implants. ASTM International, West Conshohocken
- Liepins I, Pérez A, Stroman M et al (2010) In vitro test model for evaluating fatigue performance for acetabular wedge augment device. Corpus ID: 189954330
- Fuchs J, Ron M, Liepins I et al (2011) In vitro test model for evaluating fatigue performance for acetabular wedge augment device. ORS annual meeting. Poster No. 991
- Anovitz LM, Cole DR (2015) Characterization and analysis of porosity and pore structures. *Rev Mineral Geochem* 80(1):61–164. <https://doi.org/10.2138/rmg.2015.80.04>
- Arabnejad S, Johnston RB, Pura JA et al (2016) High-strength porous biomaterials for bone replacement: a strategy to assess the interplay between cell morphology, mechanical properties, bone ingrowth and manufacturing constraints. *Acta Biomater* 30:345–356. <https://doi.org/10.1016/j.actbio.2015.10.048>